

# Residual Bound $\text{Ca}^{2+}$ Can Account for the Effects of $\text{Ca}^{2+}$ Buffers on Synaptic Facilitation

Victor Matveev, Richard Bertram and Arthur Sherman

*J Neurophysiol* 96:3389-3397, 2006. First published Sep 13, 2006; doi:10.1152/jn.00101.2006

**You might find this additional information useful...**

---

This article cites 45 articles, 26 of which you can access free at:

<http://jn.physiology.org/cgi/content/full/96/6/3389#BIBL>

Updated information and services including high-resolution figures, can be found at:

<http://jn.physiology.org/cgi/content/full/96/6/3389>

Additional material and information about *Journal of Neurophysiology* can be found at:

<http://www.the-aps.org/publications/jn>

---

This information is current as of November 17, 2006 .

# Residual Bound $\text{Ca}^{2+}$ Can Account for the Effects of $\text{Ca}^{2+}$ Buffers on Synaptic Facilitation

Victor Matveev,<sup>1</sup> Richard Bertram,<sup>2</sup> and Arthur Sherman<sup>3</sup>

<sup>1</sup>Department of Mathematical Sciences, New Jersey Institute of Technology, Newark, New Jersey; <sup>2</sup>Department of Mathematics and Programs in Neuroscience and Molecular Biophysics, Florida State University, Tallahassee, Florida; and <sup>3</sup>Laboratory of Biological Modeling, National Institute of Diabetes and Digestive and Kidney Diseases, National Institutes of Health, Bethesda, Maryland

Submitted 30 January 2006; accepted in final form 1 September 2006

**Matveev, Victor, Richard Bertram, and Arthur Sherman.** Residual bound  $\text{Ca}^{2+}$  can account for the effects of  $\text{Ca}^{2+}$  buffers on synaptic facilitation. *J Neurophysiol* 96: 3389–3397, 2006. First published September 13, 2006; doi:10.1152/jn.00101.2006. Facilitation is a transient stimulation-induced increase in synaptic response, a ubiquitous form of short-term synaptic plasticity that can regulate synaptic transmission on fast time scales. In their pioneering work, Katz and Miledi and Rahamimoff demonstrated the dependence of facilitation on presynaptic  $\text{Ca}^{2+}$  influx and proposed that facilitation results from the accumulation of residual  $\text{Ca}^{2+}$  bound to vesicle release triggers. However, this bound  $\text{Ca}^{2+}$  hypothesis appears to contradict the evidence that facilitation is reduced by exogenous  $\text{Ca}^{2+}$  buffers. This conclusion led to a widely held view that facilitation must depend solely on the accumulation of  $\text{Ca}^{2+}$  in free form. Here we consider a more realistic implementation of the bound  $\text{Ca}^{2+}$  mechanism, taking into account spatial diffusion of  $\text{Ca}^{2+}$ , and show that a model with slow  $\text{Ca}^{2+}$  unbinding steps can retain sensitivity to free residual  $\text{Ca}^{2+}$ . We demonstrate that this model agrees with the facilitation accumulation time course and its biphasic decay exhibited by the crayfish inhibitor neuromuscular junction (NMJ) and relies on fewer assumptions than the most recent variants of the free residual  $\text{Ca}^{2+}$  hypothesis. Further, we show that the bound  $\text{Ca}^{2+}$  accumulation is consistent with Kamiya and Zucker's experimental results, which revealed that photolytic liberation of a fast  $\text{Ca}^{2+}$  buffer decreases the synaptic response within milliseconds. We conclude that  $\text{Ca}^{2+}$  binding processes with slow unbinding times (tens to hundreds of milliseconds) constitute a viable mechanism of synaptic facilitation at some synapses and discuss the experimental evidence for such a mechanism.

## INTRODUCTION

Synaptic facilitation is a transient activity-dependent increase in synaptic strength, decaying on time scales from tens to hundreds of milliseconds. It is observed in a vast variety of neural systems, from invertebrate junction potentials to neocortical synapses, and, along with short-term depression, may play a role in shaping the neural population dynamics on fast time scales. Notwithstanding a few postsynaptic contributions such as temporal summation of successive excitatory postsynaptic potentials (EPSPs) at high stimulation frequencies and the depolarization-dependent relief of  $\text{Mg}^{2+}$  block of *N*-methyl-D-aspartate (NMDA) receptors at glutamatergic synapses, facilitation is primarily a presynaptic phenomenon, dependent on presynaptic  $\text{Ca}^{2+}$  entry (see reviews by Fisher et al. 1997; Magleby 1987; Zucker 1999; Zucker and Regehr 2002). Facilitation of the synaptic response may be caused for instance by the facilitation of action potential (AP)-evoked  $\text{Ca}^{2+}$  currents due to a depolarization-dependent relief of G-protein-mediated inhibition of  $\text{Ca}^{2+}$  channels (Bertram et al. 2003; Brody and Yue 2000). However, in many preparations, facilitation can be achieved even under conditions of constant pulse-to-pulse  $\text{Ca}^{2+}$  influx. This was suggested in the pioneering studies of amphibian neuromuscular junctions by Katz and Miledi (1968) and Rahamimoff (1968), who proposed that facilitation results from the accumulation of residual  $\text{Ca}^{2+}$  bound to  $\text{Ca}^{2+}$ -dependent vesicle release sensors. This so-called bound residual  $\text{Ca}^{2+}$  hypothesis of synaptic facilitation was later explored in modeling studies (Bennett et al. 1997; Bertram et al. 1996; Delaney et al. 1994; Dittman et al. 2000; Yamada and Zucker 1992). However, interest in the bound  $\text{Ca}^{2+}$  hypothesis has been limited due to experimental evidence demonstrating the reduction of facilitation by exogenous  $\text{Ca}^{2+}$  buffers. Because the main effect of exogenous buffers is to absorb the *free*  $\text{Ca}^{2+}$  ions, with no effect on  $\text{Ca}^{2+}$  that is already bound, these results have been used to argue that the free and not bound residual  $\text{Ca}^{2+}$  underlies facilitation (see review by Zucker and Regehr 2002). Notably, experiments of Kamiya and Zucker (1994) on crayfish neuromuscular junctions showed that the synaptic response is reduced within milliseconds of a UV flash photolysis of a fast  $\text{Ca}^{2+}$ -absorbing buffer diazo-2 in the presynaptic terminal, demonstrating the apparent role of residual *free*  $\text{Ca}^{2+}$  in facilitated neurotransmitter release.

Thus it is now widely accepted that synaptic facilitation is caused primarily by the gradual accumulation of *free* [ $\text{Ca}^{2+}$ ] during the conditioning train of stimuli (Zucker and Regehr 2002). One mechanism for this is the facilitation of AP-evoked  $\text{Ca}^{2+}$  transients caused by the gradual saturation of endogenous buffers during continued stimulation. Proposed on purely theoretical grounds (Klingauf and Neher 1997; Neher 1998), this buffer saturation mechanism was recently shown to underlie facilitation at calbindin-positive neocortical and hippocampal synapses (Blatow et al. 2003; see also Jackson and Redman 2003; Maeda et al. 1999; Rozov et al. 2001). Recent modeling results indicate that a dramatic increase in  $\text{Ca}^{2+}$  transients can be achieved if buffers saturate in the entire presynaptic terminal, which requires optimal concentrations of fast mobile buffers similar to calbindin (Matveev et al. 2004).

Alternatively, if endogenous buffers are primarily immobile and are present in sufficiently large concentrations, they will

Address for reprint requests and other correspondence: V. Matveev, New Jersey Institute of Technology, University Heights, Newark, NJ 07102 (E-mail: matveev@oak.njit.edu).

The costs of publication of this article were defrayed in part by the payment of page charges. The article must therefore be hereby marked "advertisement" in accordance with 18 U.S.C. Section 1734 solely to indicate this fact.

mostly saturate *locally*, within a  $\text{Ca}^{2+}$  channel nanodomain, trapping  $\text{Ca}^{2+}$  that enters during a stimulus and then slowly releasing it during interstimulus intervals (Neher 1998; Nowycky and Pinter 1993; Sala and Hernández-Cruz 1990). This would lead to accumulation in *residual* free  $\text{Ca}^{2+}$  after each action potential in addition to some increase in  $\text{Ca}^{2+}$  transients associated with the local buffer saturation. Recent modeling studies (Matveev et al. 2002; Tang et al. 2000; see also Bennett et al. 2004) have shown that such a free residual  $\text{Ca}^{2+}$  mechanism of facilitation incorporating two spatially segregated  $\text{Ca}^{2+}$  binding sites can explain the magnitude and the time course of facilitation growth observed at the crayfish neuromuscular junction (NMJ). However, this two-site free- $\text{Ca}^{2+}$  model requires a number of assumptions to match the experimental data, such as high tortuosity of the intracellular space close to the  $\text{Ca}^{2+}$  channel, the immobilization of exogenous  $\text{Ca}^{2+}$  buffers by the cytoskeleton, and a significant spatial separation ( $>150$  nm) between two distinct release-controlling  $\text{Ca}^{2+}$ -binding sites (both of which must be occupied for release to occur).

Thus recent modeling studies focused on the role of *free*  $\text{Ca}^{2+}$  in facilitation, based on the conclusion that the contribution of bound  $\text{Ca}^{2+}$  to facilitation, is ruled out by the experimentally observed sensitivity of facilitation to exogenous  $\text{Ca}^{2+}$  buffers. However, as we show in the following text, this conclusion is unjustified. Further, it explicitly rules out the contribution of slow processes involving priming and/or docking of synaptic vesicles (see DISCUSSION) (see also Millar et al. 2005) because such processes cannot instantly reach equilibrium with the changing intracellular  $\text{Ca}^{2+}$  concentration and may not be described by a model that only takes into account free  $\text{Ca}^{2+}$ . Therefore we revisit the *bound* residual  $\text{Ca}^{2+}$  hypothesis of facilitation and show that its biophysically realistic implementation that takes into account the diffusion and buffering of  $\text{Ca}^{2+}$  can also account for the properties of the synaptic response recorded in the crayfish inhibitor NMJ. Moreover, we find that this model requires fewer assumptions than the abovementioned two-site mechanism. We show that it can be easily reconciled with the observed effect of exogenous  $\text{Ca}^{2+}$  buffers on synaptic response. Importantly, the model we present can readily account for several additional experimentally observed features of synaptic facilitation. For example, the same experiments that revealed the sensitivity of facilitation to exogenous buffers also uncovered a component of release whose decay lagged behind the decay of free residual  $[\text{Ca}^{2+}]$  (Atluri and Regehr 1996; Kamiya and Zucker 1994), suggesting that residual bound  $\text{Ca}^{2+}$  is one component of facilitation (see also Dittman et al. 2000; Regehr et al. 1994). Further, our model easily accounts for the super-linear facilitation accumulation and its biphasic decay observed in a variety of synapses, and at the crayfish NMJ in particular (Tang et al. 2000). Therefore we believe that current experimental evidence does not rule out the involvement in facilitation of processes characterized by slow  $\text{Ca}^{2+}$  unbinding with unbinding time scales of tens of milliseconds and above.

## METHODS

We first solve the partial differential equations describing the diffusion and mutual binding of  $\text{Ca}^{2+}$  ions and buffer molecules (Eqs. 1–5). We then use the resulting  $\text{Ca}^{2+}$  concentration time course to

drive the kinetic scheme modeling the binding of  $\text{Ca}^{2+}$  to vesicle release triggers (Eqs. 6 and 7). The simulated synaptic response is given directly in terms of the occupancy of the final “R” release state in the scheme described by Eqs. 8 and 9 (see Fig. 2F). We are interested in comparing our bound residual  $\text{Ca}^{2+}$  model results with those of the two-site free residual  $\text{Ca}^{2+}$  model; therefore our model shares some of its features, in particular the geometry of the active zone, with the model of Matveev et al. (2002), which in turn is based on the work of Tang et al. (2000). These models are adapted to a specific experimental system, the crayfish inhibitor NMJ, which exhibits very pronounced facilitation not occluded by concomitant synaptic depression, making it a perfect system for the study of synaptic facilitation.

## Equations describing buffered diffusion of $\text{Ca}^{2+}$

We assume that the binding of  $\text{Ca}^{2+}$  to both the endogenous and the exogenous buffers is described by simple mass action kinetics with one-to-one stoichiometry



where  $k_j^{\text{on}}$  and  $k_j^{\text{off}}$  are, respectively, the binding and the unbinding rates of the  $j$ th  $\text{Ca}^{2+}$  buffer species,  $B_j$ . This leads to the following reaction-diffusion equations for the  $\text{Ca}^{2+}$  concentration, and the concentrations of the free (unbound) buffers

$$\frac{\partial[\text{Ca}^{2+}]}{\partial t} = D_{\text{Ca}} \nabla^2[\text{Ca}^{2+}] + \sum_{j=1}^{N_{\text{buffers}}} R_j([\text{Ca}^{2+}], [B_j]) + \frac{1}{2F} I_{\text{Ca}}(t) \sum_{i=1}^{N_{\text{channels}}} \delta(r - r_i) \quad (2)$$

$$\frac{\partial[B_j]}{\partial t} = D_j \nabla^2[B_j] + R_j([\text{Ca}^{2+}], [B_j]) \quad (3)$$

where  $R_j$  is the reaction term describing the mass-action kinetics given by scheme 1

$$R_j([\text{Ca}], [B_j]) = -k_j^{\text{on}}[\text{Ca}^{2+}][B_j] + k_j^{\text{off}}(B_j^{\text{total}} - [B_j]) \quad (4)$$

$B_j^{\text{total}}$  denotes the total concentration of the  $j$ th buffer;  $D_j$  and  $D_{\text{Ca}}$  are the diffusion coefficients in cytosol of the  $j$ th buffer and  $\text{Ca}^{2+}$ , respectively. We choose  $D_{\text{Ca}} = 0.2 \mu\text{m}^2 \text{ms}^{-1}$  (Allbritton et al. 1992). Following standard convention, in Eqs. 2 and 3, we have assumed that the initial distribution of the buffer is spatially uniform and that the diffusion coefficient of the buffer is not affected by the binding of  $\text{Ca}^{2+}$ . Under these assumptions, the sum of the bound and the unbound buffer concentrations is constant in space and time and is equal to the total buffer concentration,  $B_j^{\text{total}}$ . Thus  $[\text{Ca}B_j] = B_j^{\text{total}} - [B_j]$ . The last term in Eq. 2 represents the  $\text{Ca}^{2+}$  influx, where  $F$  is Faraday’s constant,  $I_{\text{Ca}}(t)$  is the (inward) calcium current per channel (see following text), and  $\delta(r - r_i)$  is the Dirac delta function centered at the location of the  $i$ th channel.

Recent experiments of Lin et al. (2005) indicate that crayfish NMJ terminals contain two distinct endogenous buffer classes, one of which is characterized by slow  $\text{Ca}^{2+}$  unbinding kinetics ( $k_{\text{slow}}^{\text{off}} = 0.1\text{--}1 \text{ s}^{-1}$ ). Similar buffering systems are found in central mammalian synapses, for instance in rodent Purkinje cells, which contain a slow buffer parvalbumin along with the fast-binding calbindin (Schmidt et al. 2003). Therefore we assume that two endogenous buffer species are present, one of which is characterized by slow  $\text{Ca}^{2+}$  binding kinetics, with an unbinding rate of  $k_{\text{slow}}^{\text{off}} = 0.4 \text{ s}^{-1}$  and an affinity of  $K_D^{\text{slow}} = 5 \mu\text{M}$ . For simplicity, we assume that both buffers have the same mobility,  $D_B$ , assumed to be a free quantity with respect to the parameter sensitivity analysis presented in Fig. 6. The  $\text{Ca}^{2+}$ -binding characteristics and the binding ratio of the fast buffer,  $\kappa_0^{\text{fast}}$ , are considered to be free parameters, while the capacity of the slow buffer is constrained to yield a total resting  $\text{Ca}^{2+}$ -binding ratio of 600, as

TABLE 1. Free model parameters and the set of values used in the parameter sensitivity analysis shown in Fig. 6

Symbol	Parameter Name	Set of Values
$Q_{Ca}$	$Ca^{2+}$ influx per channel per AP	0.065, 0.13, <b>0.26</b> , 0.39, 0.65 (pA · ms)
$\kappa_0^{fast}$	Resting capacity of fast buffer	<b>50</b> , 100, 200, 300
$K_D^{fast}$	$Ca^{2+}$ affinity of fast buffer	0.2, 0.5, 1, 2, 5, <b>10</b> ( $\mu M$ )
$D_B$	Endogenous buffer mobility	0, $10^{-4}$ , $10^{-3}$ , $3 \cdot 10^{-3}$ , $10^{-2}$ , <b><math>3 \cdot 10^{-2}</math></b> , 0.1 ( $\mu m^2/ms$ )
$d^{XY}$	Distance from the center of active zone	<b>130</b> , 150, 170, 190 (nm)
$K_D^{XY}$	$Ca^{2+}$ affinity of X and Y sites	5, 10, <b>20</b> , 30 ( $\mu M$ )

Numbers labeled in *bold* indicate the reference parameter set used for simulations in Figs. 2–5. The resting buffer capacity is defined as the ratio of total concentration to its affinity ( $\kappa_0^{fast} = B_{fast}^{Total}/K_D^{fast}$ ). The slow buffer's parameters are:  $k_{slow}^{off} = 0.4 s^{-1}$ ,  $K_D^{slow} = 5 \mu M$ ,  $\kappa_0^{slow} = 600 - \kappa_0^{fast}$ . AP, action potential.

estimated by Tank et al. (1995):  $\kappa_0^{slow} = 600 - \kappa_0^{fast}$ . The results are more sensitive to  $\kappa_0^{fast}$  than to  $\kappa_0^{slow}$  and are only slightly affected if the total binding ratio is varied between 300 and 800 given a fixed value of  $\kappa_0^{fast}$ . The list of free parameters is summarized in Table 1. The reference set of values shown in bold is used in the simulations presented in Figs. 2–5. Exogenous buffers fura-2 and diazo-2 are assumed to be mobile ( $D_{fura} = 118 \mu m^2 ms^{-1}$ ,  $D_{diazo} = 100 \mu m^2 ms^{-1}$ ); their parameters are given in the captions to Figs. 3 and 4.

Equations 2–4 are solved inside a box enclosure representing the volume surrounding a single active zone of a crayfish nerve terminal (Fig. 1). Using the symmetry assumption, we only model a quarter of this elementary volume (dashed box in Fig. 1), as a box with dimensions  $0.8 \times 0.8 \times 1 \mu m^3$ . We assume 16  $Ca^{2+}$  channels per active zone or 4 channels in our enclosure representing a quarter of an active zone. Following Tang et al. (2000) and Matveev et al. (2002), each AP is modeled as a 1-ms-long constant  $Ca^{2+}$  current,  $I_{Ca}^{AP}$ , followed by a 3.5-fold larger 0.2-ms-long tail current entering through each of the  $Ca^{2+}$  channels,  $I_{Ca}^{tail} = 3.5 I_{Ca}^{AP}$ . Given the large uncertainty in the value of single-channel  $Ca^{2+}$  influx (Tang et al. 2000; Tank et al. 1995), we consider  $I_{Ca}^{AP}$  to be a free model parameter, varying over the range 0.04–0.4 pA. This yields a total  $Ca^{2+}$  influx per channel per action potential in the range  $Q_{Ca} = 0.065$ – $0.65 pA \cdot ms$  (see Table 1).

We impose reflective boundary conditions for  $Ca^{2+}$  and buffer(s) on the sides of the box, thereby assuming that the  $Ca^{2+}$  and buffer fluxes flowing into the enclosure from the neighboring AZ regions are balanced by the equal fluxes flowing out of the enclosure. The boundary condition for  $[Ca^{2+}]$  on the top and bottom surfaces relates the flux to the local  $Ca^{2+}$  concentration, simulating extrusion by surface pumps

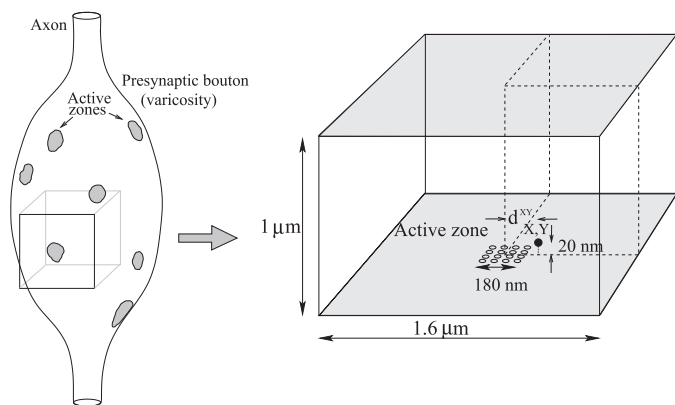


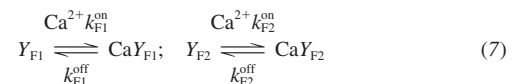
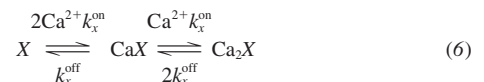
FIG. 1. Simulation volume (*right*) approximates the volume surrounding a single active zone of a crayfish presynaptic varicosity (*left*). Assuming symmetry of the geometry with respect to 2 mutually perpendicular vertical planes, only 1/4 of the total volume is considered (dashed lines). Boundary conditions on all side surfaces are 0-flux, whereas boundary conditions on the bottom and top surfaces take into account outward flux due to  $Ca^{2+}$  extrusion (Eq. 5). ○, positions of  $Ca^{2+}$  channels (16 per active zone); ●, position of the X and Y  $Ca^{2+}$  binding sites for simulations shown in Figs. 2–5. This site is located 20 nm above the membrane, at a distance of  $d^{XY} = 130$  nm from the center of the active zone (~55 nm away from the nearest  $Ca^{2+}$  channel).

$$\frac{\partial [Ca^{2+}]}{\partial n} + \frac{M}{D_{Ca}} \frac{[Ca^{2+}]}{[Ca^{2+}] + K_p} - f_{leak} = 0 \tag{5}$$

Here  $\partial/\partial n \equiv n \cdot \nabla$  denotes differentiation in the direction normal to the boundary;  $M$  is the maximal pump rate,  $K_p$  is the pump dissociation constant, and  $f_{leak}$  is the  $Ca^{2+}$  leak term that is tuned to yield zero pump rate at rest:  $f_{leak} = (M/D_{Ca}) [Ca^{2+}]_{bgr}/([Ca^{2+}]_{bgr} + K_p)$ , where  $[Ca^{2+}]_{bgr} = 0.05 \mu M$  is the resting background  $[Ca^{2+}]$ . We use values of  $K_p = 0.4 \mu M$  (Carafoli 1987; Dipolo and Beauge 1983) and  $M = 0.04 \mu M \mu m ms^{-1}$ . At low  $[Ca^{2+}]$ , this yields a  $Ca^{2+}$  clearance time constant of  $\tau \approx (1 + \kappa_0) V (K_p + [Ca^{2+}]_{bgr})^2 / (K_p M S) \approx 4 s$ , where  $V$  and  $S$  are the volume and the surface area of the bouton (Fig. 1), and  $\kappa_0 = 600$  is the resting total endogenous buffering capacity at the crayfish NMJ. This pump rate is consistent with the experimental estimates of Tank et al. (1995).

### $Ca^{2+}$ binding and synaptic response

The understanding of the fast  $Ca^{2+}$ -triggered vesicle fusion is still incomplete. A promising candidate mechanism is provided by the  $Ca^{2+}$ -dependent interaction of synaptotagmin I with phospholipids and the SNARE complex (reviewed by Chapman 2002; Koh and Bellen 2003). The molecular identity of the putative facilitation sensor is also uncertain, although recent evidence suggests the involvement of the neuronal  $Ca^{2+}$  sensor class of proteins, namely NCS-1 (Sippy et al. 2003) and its crustacean and *Drosophila* homologue, frequenin (Jeromin et al. 1999). In both cases, the exact molecular steps involved and the physiological affinities of the corresponding  $Ca^{2+}$ -binding sites are unknown. Therefore we follow earlier work in the field and model the  $Ca^{2+}$  dependence of synaptic response via a phenomenological model that is tuned to reproduce the dynamics of synaptic response to trains of action potentials. Our  $Ca^{2+}$  binding scheme is similar to the one used in Yamada and Zucker (1992), Tang et al. (2000), and Matveev et al. (2002). It assumes the existence of two types of  $Ca^{2+}$  binding sites, X and Y, characterized by fast and slow unbinding rates, respectively. Further, to reproduce the biphasic F1/F2 decay time course of synaptic facilitation (see Fig. 5), we follow the approach of Bertram et al. (1996), and assume the presence of two distinct Y-type  $Ca^{2+}$  binding sites,  $Y_{F1}$  and  $Y_{F2}$



These reactions are driven by the  $Ca^{2+}$  time course found by integrating Eqs. 2–5; the unbinding rates of the three sites are set to  $k_x^{off} = 50 ms^{-1}$ ,  $k_{F1}^{off} = 33 s^{-1}$ , and  $k_{F2}^{off} = 3.3 s^{-1}$ . The latter two unbinding rates correspond to the F1 and F2 facilitation decay components. The  $k_{F1}^{off}$  rate yields a time constant of 30 ms, close to the F1 decay time

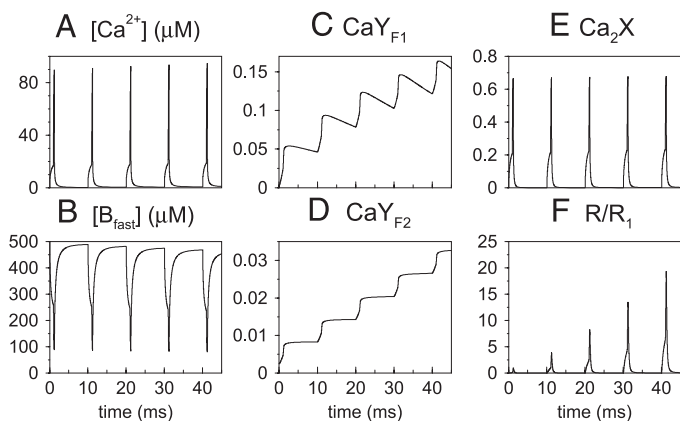
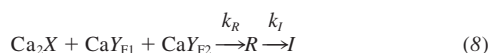


FIG. 2. Response of the model to a 100-Hz train of 5 action potentials. *A* and *B*:  $\text{Ca}^{2+}$  and fast buffer concentration time course at the release site labeled in Fig. 1. *C* and *D*: binding fractions of the faster ( $Y_{F1}$ ) and slower ( $Y_{F2}$ ) facilitatory  $\text{Ca}^{2+}$  sensors. *E*: binding fraction of the fast secretory  $X$  sensor. *F*: synaptic response normalized to its peak magnitude during the 1st pulse,  $R_1$ . Facilitation is caused by the increase in the binding of the 2  $Y$  sites (*C* and *D*) with very slight contribution of facilitation of  $\text{Ca}^{2+}$  transients (seen in *A*) due to buffer saturation, further increasing the  $Y$ -sites binding. The values of free model parameters used in this simulation are listed in bold in Table 1.

scale of  $19 \pm 5$  (SD) ms measured at the crayfish NMJ by Tang et al. (2000) and Vyshedskiy and Lin (1997), whereas the F2 decay rate is chosen to match the decay time course of synaptic response shown in Fig. 4A, as measured by Kamiya and Zucker (1994). The corresponding F2 time scale of 300 ms is somewhat shorter than the F2 time scale of  $530 \pm 200$  ms measured by Tang et al. (2000) and Vyshedskiy and Lin (1997). The binding rates of  $X$  and  $Y$  sites are determined from their affinities, which we consider to be free model parameters (see Table 1).

Reactions 6 and 7 are converted to ordinary differential equations using the law of mass action. The binding of all three sites is necessary to trigger release, schematically described by



where  $R$  is the release state, and  $I$  is the inactivated state of the release machinery. This leads to the following differential equation for  $R$ , which determines the release rate

$$\frac{dR}{dt} = k_R \text{Ca}_2\text{X} \text{CaY}_{F1} \text{CaY}_{F2} - k_I R \quad (9)$$

where

$$k_R = 1 \text{ ms}^{-1} \text{ and } k_I = 10 \text{ ms}^{-1}$$

Contrary to the two-site residual free  $\text{Ca}^{2+}$  model of synaptic facilitation (Matveev et al. 2002; Tang et al. 2000), we assume that both the  $X$  and the  $Y$  sensors are colocalized in space, and therefore the same  $[\text{Ca}^{2+}]$  signal determines the forward rates of binding described by Eqs. 6 and 7. Facilitation is defined as the ratio of the peak value of  $R$  achieved during the  $n$ th action potential, divided by the first peak response, and normalized to zero in the absence of synaptic enhancement:  $F_n = R_n/R_1 - 1$  (Figs. 3, A and B, and 5, A and B). Results would not be significantly affected if postsynaptic response and facilitation were defined in terms of a time-filtered (integrated) value of  $R$ .

We note that there may be alternative ways to implement the biphasic facilitation decay time course not involving two sites with distinct  $\text{Ca}^{2+}$ -binding kinetics. For instance, it is conceivable that the two decay time scales may correspond to the kinetics of two sequential state transitions of the facilitation site, activated downstream of  $\text{Ca}^{2+}$  binding. However, the model given by Eqs. 6–9 is the simplest

scheme that yields both a biphasic decay and a super-linear accumulation time course of synaptic facilitation.

### Numerical simulations

All simulations were performed using the CalC (“calcium calculator”) software developed by one of us (Matveev). CalC uses the alternating-direction implicit finite-difference method to solve the buffered diffusion equations (Eqs. 2–4) with second-order accuracy in spatial and temporal resolution. To preserve the accuracy of the method in the presence of the nonlinear buffering term, equations for  $[\text{Ca}^{2+}]$  and  $[B]$  are solved on separate time grids, shifted with respect to each other by half a time step. CalC uses an adaptive time-step method with a nonuniform spatial grid that has greater density of points close to the  $\text{Ca}^{2+}$  channel array. Grid size is adjusted to limit the numerical error to  $\sim 5\%$  (grid of  $34 \times 34 \times 40$  points). CalC integrates the ordinary differential equations (Eqs. 6–9) using the fourth-order adaptive Runge-Kutta method. CalC is freely available from <http://web.njit.edu/~matveev/calc.html>, and runs on all commonly used computational platforms (UNIX, including Mac OS X, and Windows/Intel). To ensure reproducibility of this work, the commented simulation script files generating the data reported here are available at the CalC web site.

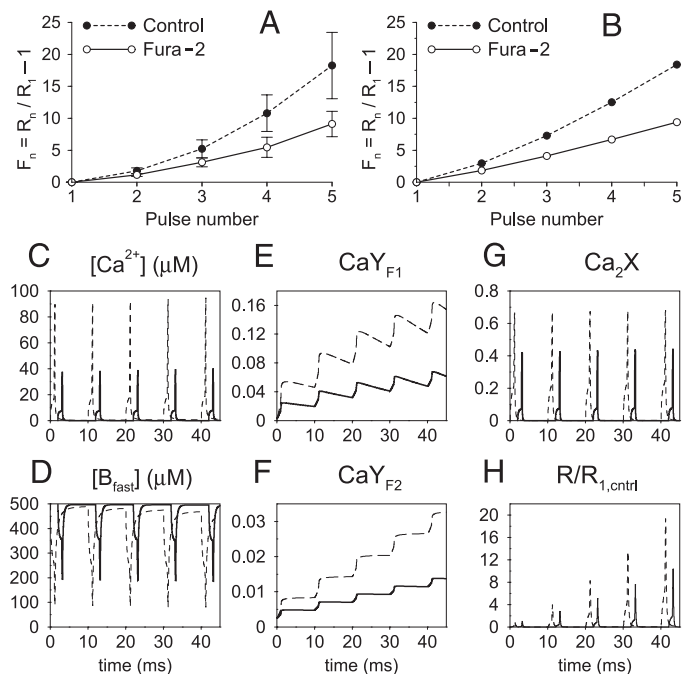


FIG. 3. Effect of exogenous buffer application on synaptic response to a 5-pulse stimulation train. *A*: experimentally measured facilitation time course in the crayfish neuromuscular junction (NMJ) with and without  $400 \mu\text{M}$  fura-2. Reproduced from Tang et al. (2000) (see Fig. 2C therein). *B*: simulation results: peak model response evoked by each of the 5 action potentials,  $R_n$ , normalized to the 1st peak response,  $R_1$ , minus one, with and without the simulated addition of  $400 \mu\text{M}$  fura-2. *Bottom*: time courses of  $\text{Ca}^{2+}$  concentration (*C*), fast buffer concentration (*D*),  $Y_{F1}$ -binding site occupancy (*E*),  $Y_{F2}$ -binding site occupancy (*F*),  $X$ -binding site occupancy (*G*), and response  $R$  (*H*), with (—) and without fura-2 (---; same as in Fig. 2, A–F). In *H*, response is normalized to the 1st peak response in the absence of fura-2,  $R_{1,\text{ctrl}}$ . Fura-2 results in *C*, *D*, *G*, and *H* are shifted to the right by 2 ms for easier comparison with the control curves. The properties of the buffer simulating fura-2 ( $K_D = 360 \text{ nM}$ ,  $D = 118 \mu\text{m}^2 \text{ s}^{-1}$ , unbinding rate =  $96.7 \text{ s}^{-1}$ ,  $[\text{Fura-2}]_{\text{total}} = 400 \mu\text{M}$ ) are the same as in Tang et al. (2000). Note that part of fura-2 is  $\text{Ca}^{2+}$ -bound at the beginning of the simulation, to yield a background  $[\text{Ca}^{2+}]$  of  $50 \text{ nM}$ . Other parameters same as in Fig. 2 (see Table 1).

## RESULTS

*Response to a five-pulse train of action potentials*

Figure 2 demonstrates the response of the synaptic model when it is driven by a train of five simulated action potentials ( $\text{Ca}^{2+}$  current pulses), delivered at 100 Hz. Facilitation of release shown in *F* results from accumulation of  $\text{Ca}^{2+}$  bound to the two *Y* sites (Eq. 7) throughout the train of action potentials (Fig. 2, *C* and *D*). This accumulation is caused by the slow unbinding of  $\text{Ca}^{2+}$  from the  $Y_{F1}$  and  $Y_{F2}$  sites so that binding that occurs during one stimulus is only partially removed before the next stimulus. Examination of the  $\text{Ca}^{2+}$  and buffer concentration time courses given in *A* and *B* also reveals a very slight increase in  $\text{Ca}^{2+}$  transients associated with the saturation of the  $\text{Ca}^{2+}$  buffer. It makes only a negligible contribution to facilitation, slightly increasing the pulse-to-pulse growth in  $\text{Ca}^{2+}$  binding to the *X* and *Y* sites (see DISCUSSION).

Importantly, both the magnitude and the super-linear, non-saturating time course of facilitation are in good agreement with the experimental results of Tang et al. (2000), reproduced in Fig. 3*A* (control curve). This super linearity was achieved with no additional assumptions, contrary to the two-site mechanism (cf. Fig. 2 of Matveev et al. 2002). In particular, tortuosity (retardation of diffusion close to the membrane) was not included in the present model, and the two  $\text{Ca}^{2+}$  binding sites are *not* spatially segregated, but located at the same distance (55 nm) from the nearest  $\text{Ca}^{2+}$  channel.

*Facilitation is reduced in the presence of exogenous  $\text{Ca}^{2+}$  buffers*

One of our main goals is to explore the sensitivity of a model with slow  $\text{Ca}^{2+}$  unbinding steps to changes in intracellular buffering capacity. Experimental results of Tang et al. (2000) are shown in Fig. 3*A* and suggest that facilitation is reduced about twofold on injection of 400  $\mu\text{M}$  of the  $\text{Ca}^{2+}$  indicator dye fura-2 into the crayfish NMJ. We mimic this experiment by repeating the simulations shown in Fig. 2 after including in our model (Eqs. 2 and 3) 400  $\mu\text{M}$  of a fura-2-like buffer. Because the background [ $\text{Ca}^{2+}$ ] should remain unchanged after the newly introduced buffer equilibrates with the intracellular  $\text{Ca}^{2+}$  homeostasis processes, in our simulations, the fura-2 buffer is assumed to be partially  $\text{Ca}^{2+}$  bound at rest, so that the background [ $\text{Ca}^{2+}$ ] remains constant at 0.05  $\mu\text{M}$ . Simulation results presented in Fig. 3*B* show a reduction of facilitation to a degree comparable to that observed experimentally. This reduction is caused by the decrease in the free [ $\text{Ca}^{2+}$ ] in the vicinity of the *X* and *Y* binding sites (Fig. 3*C*), leading to a reduction in the amount of binding achieved during each action potential (Fig. 3, *E–G*). Thus even though additional buffers cannot accelerate the unbinding of  $\text{Ca}^{2+}$  from the *Y* sites, the reduction in the free ambient [ $\text{Ca}^{2+}$ ] caused by the added  $\text{Ca}^{2+}$  buffers is sufficient to reduce the magnitude of synaptic facilitation, demonstrating the sensitivity of the model to free [ $\text{Ca}^{2+}$ ].

Although the variation of the two-site residual free  $\text{Ca}^{2+}$  model considered by Matveev et al. (2002) was also successful in reproducing the twofold reduction of facilitation shown in Fig. 3, such agreement required an assumption of almost complete immobilization of the indicator dye in the entire presynaptic terminal. This is because a fast mobile buffer is

extremely efficient in reducing the residual  $\text{Ca}^{2+}$  at a remote facilitation site and would predict a much more dramatic effect of fura-2 on facilitation than seen experimentally. In contrast, the model we present here does not impose any constraints on the diffusion of the fura-2, which is assumed to have a diffusion coefficient of  $D_{F2} = 118 \mu\text{m}^2/\text{s}$  (Gabso et al. 1997). Further, the two-site model also required an assumption of significant tortuosity retarding  $\text{Ca}^{2+}$  diffusion in a 200-nm side layer proximal to the membrane, to achieve a nonsaturating facilitation accumulation time course. Again, this assumption is not necessary in the present model, where the super-linearity is caused by the accumulation of bound  $\text{Ca}^{2+}$ .

 *$\text{Ca}^{2+}$  buffering rapidly reduces facilitated response*

A crucial experiment testing the sensitivity of neurotransmitter release to free  $\text{Ca}^{2+}$  was performed by Kamiya and Zucker (1994), who measured the effect of a rapid increase in intracellular buffering capacity on facilitated synaptic response, using flash photolysis of the caged  $\text{Ca}^{2+}$  buffer diazo-2. The UV flash increases the  $\text{Ca}^{2+}$  affinity of diazo-2, resulting in a rapid sequestering of free  $\text{Ca}^{2+}$ . When the UV flash was applied after a facilitating train of pulses, the synaptic response to a test pulse administered 10 ms after the flash was reduced dramatically as compared with the control no-flash condition (Fig. 4*A*). This has been interpreted to suggest that the facilitation of neurotransmitter release is rapidly reduced when the free  $\text{Ca}^{2+}$  is buffered. Figure 4*B* demonstrates that our model reproduces these experimental observations. As shown in Fig. 4, *C–F*, diazo-2 rapidly buffers the free  $\text{Ca}^{2+}$ , reducing binding to both the *X* and the *Y* gates. The reduction in the binding of the  $Y_{F1}$  site contributes the most to the overall reduction of response. Because the *X* site has even faster kinetics, it is partially saturated by the peak  $\text{Ca}^{2+}$  transient even with diazo-2 present, limiting its impact, as compared with the  $Y_{F1}$  site. Binding of the  $Y_{F2}$  site on the other hand is too slow to contribute significantly to the reduction of the first test response (Fig. 4*E*) and has more impact on later test responses (note the difference in time scales in *C–E*). The binding of the  $Y_{F2}$  sensor is reduced by only 6% at the peak of the first test pulse, as compared with a 32% reduction in the binding of the  $Y_{F1}$  site (Fig. 4*D*), and a 18% reduction in the binding of the *X* site (Fig. 4*C*).

Thus in our model diazo-2 has two effects: it reduces the unfacilitated, baseline synaptic response, which is primarily controlled by the *X* and the  $Y_{F1}$  sites, and it also decreases facilitation by reducing the binding of the  $Y_{F1}$  and the  $Y_{F2}$  sites. Both in the experiment and in our model, diazo-2 does not completely eliminate facilitation during the 10-ms-long interval between the UV flash and the first test pulse. In the model, this is due to the slow unbinding of the *Y* gates. In fact, the decay of facilitation lags significantly behind the decay of residual free  $\text{Ca}^{2+}$  (cf. Fig. 4, *F* and *D* and *E*), in agreement with the results of Kamiya and Zucker (see Fig. 4 therein) and consistent with experiments of Atluri and Regehr (1996).

Note that the reduction in response caused by the photolyzed diazo-2 gradually dissipates within a second after the UV flash, contrary to the prediction of our model (cf. Fig. 4, *A* and *B*). We suggest that such experimentally observed reduction of the

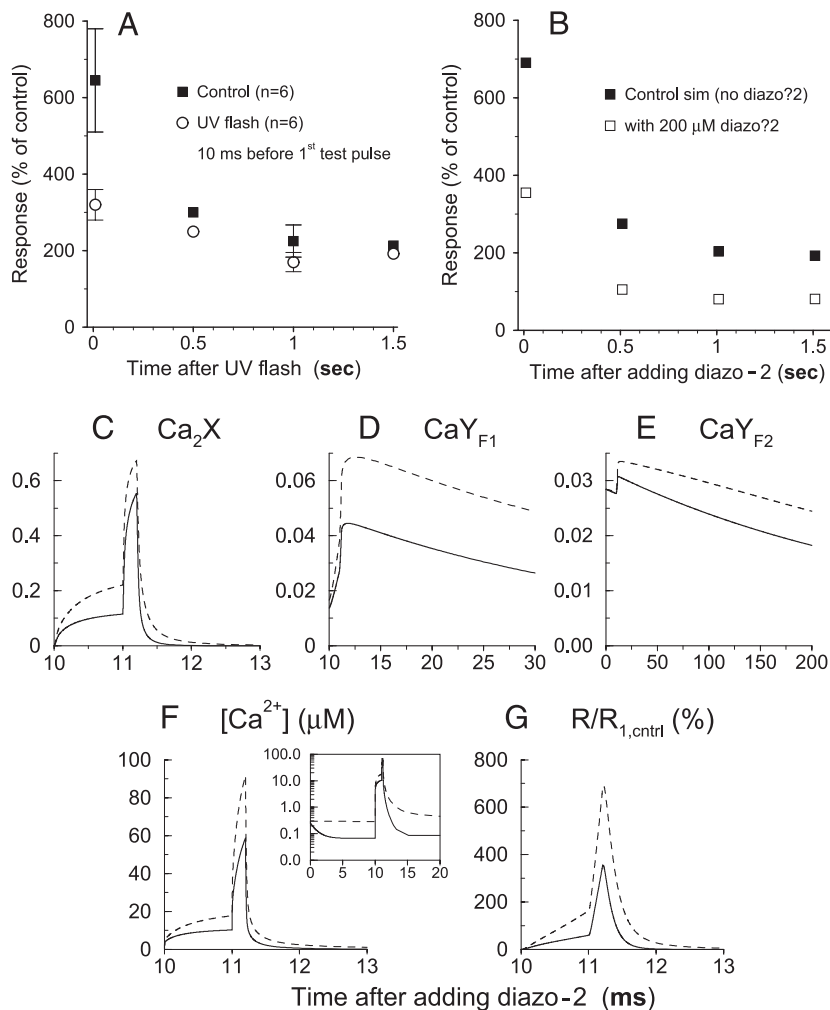


FIG. 4. Synaptic response is reduced rapidly on photolysis of a caged  $Ca^{2+}$  buffer diazo-2. *A*: experimental results of Kamiya and Zucker (1994), showing the amplitudes of synaptic responses to several test pulses administered at different times following a conditioning train of 10 action potentials (APs), normalized to the peak response during the 1st AP in the conditioning train (not shown). The 1st test pulse is applied 10 ms after a UV flash which increases the  $Ca^{2+}$  affinity of the diazo-2 buffer, sequestering  $Ca^{2+}$ . *B*: simulation of the experiment shown in *A*, showing the peak model response to test pulses administered 200 ms after a conditioning train of 5 APs applied at 100 Hz, normalized to the peak response to the 1st (unfacilitated) AP. The UV flash is simulated by adding to our model 200  $\mu$ M of diazo-2-like buffer with affinity of 150 nM, at 10 ms before the 1st test pulse. In contrast to simulations in Fig. 3, all of the buffer is added in  $Ca^{2+}$ -free form. *Bottom*: effect of adding diazo-2 on the model's response to the 1st test pulse: the time courses of binding of the secretory X-site (*C*), binding of the  $Y_{F1}$ -site (*D*), binding of the  $Y_{F2}$ -site (*E*),  $Ca^{2+}$  concentration (*F*), and synaptic response (*G*), normalized to peak response to the 1st pulse in the stimulating train. ---, control simulation; —, diazo-2 simulation. The inset in *F* shows  $[Ca^{2+}]$  time course using a logarithmic scale to demonstrate more clearly the buffering effect of diazo-2 before and after the 1st test pulse is administered at  $t = 10$  ms. Note the difference in time scales among panels. Model parameters are the same as in Figs. 2 and 3.

diazo-2 effect may be caused either by the leak of diazo-2 into the axon or a reduction in its  $Ca^{2+}$  affinity because under conditions of constant diazo-2 concentration, the response should not approach its value in the absence of the exogenous buffer.

#### Facilitation decay time course

Because facilitation is defined in terms of the relaxation time scale of the enhanced response back to its prestimulation level, it is important to examine the decay time course of the model facilitation. Figure 5*A* demonstrates the decrease of synaptic response to the last pulse in a five-pulse train as the interval between the last two pulses is increased under control conditions and in the presence of 400  $\mu$ M of

fura-2, measured by Tang et al. (2000). Figure 5*B* presents the corresponding simulation results. The first data point corresponds to an interpulse interval of 10 ms and therefore matches the five-pulse facilitation magnitude shown in Fig. 3. Note that the biphasic decay time course of facilitation is captured by the bound- $Ca^{2+}$  model. In the simulation, the time scales of both phases are determined by the rate of  $Ca^{2+}$  unbinding from the two  $Y$  gates. The model decay is faster than the one seen in experiment because the  $k_{F2}^{off}$  binding rate was adjusted to fit the decay time course of facilitation shown in Fig. 4*B*, recorded in an independent set of experiments by Kamiya and Zucker (1994). The decay time scale of the two phases can be easily adjusted by varying  $k_{F1}^{off}$  and  $k_{F2}^{off}$ . At present no other biophysical facil-

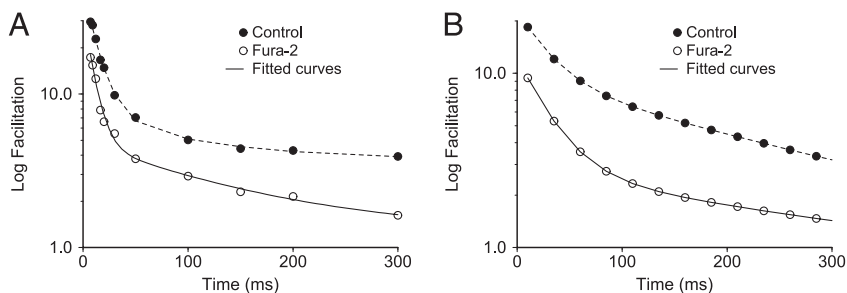


FIG. 5. Decay time course of facilitated synaptic response as a function of the last inter-spike interval in a 5-pulse stimulation train. *A*: experimental data of Tang et al. (2000) (see Fig. 3*B* therein). *B*: simulated facilitation decay time course. Note that the experimentally observed biphasic decay of facilitation is captured by the model. All parameter values are the same as in Figs. 2-4.

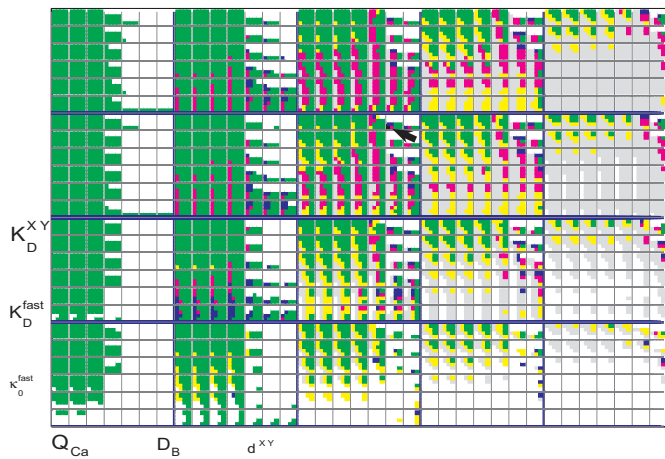


FIG. 6. The dependence of facilitation accumulation time course on 6 free model parameters listed in Table 1, presented using the dimensional stacking method. The fit between model and experiment is indicated in color code. See text for the description of dimensional stacking. The black arrow points to the reference parameter set (black pixel) used in Figs. 2–5 and shown in bold in Table 1. Note that the concentration of the fast buffer is proportional to  $K_D^{\text{fast}}$  given a fixed value of  $\kappa_0^{\text{fast}}$ .

itation model can readily explain the biphasic nature of facilitation decay.

#### Parameter sensitivity analysis

Because many of the model parameters are either unconstrained or poorly constrained by existing experimental data, it is instructive to analyze the parameter sensitivity of the fit between model and experiment. Given the large number of parameters, we employ a technique called dimensional stacking (Taylor et al. 2006). Results presented in Fig. 6 show the dependence of facilitation accumulation properties indicated in color code as explained in the following text as a function of the following quantities: 1) the  $\text{Ca}^{2+}$  affinities of the X and Y sites,  $K_D^{XY}$ . Because the variation of any of these affinities affects the results in a similar way, regulating the saturation level of the corresponding site, for the sake of simplicity these are set to be equal. 2) The  $\text{Ca}^{2+}$  influx per action potential per active zone,  $Q_{\text{Ca}}$ . 3) The mobility of the endogenous buffers,  $D_B$ . We assume that both buffers have equal diffusion coefficients. 4) The affinity of the fast buffer,  $K_D^{\text{fast}}$ . Because the buffering capacity of the buffer is varied independently (see next parameter), the total concentration of the fast buffer is proportional to  $K_D^{\text{fast}}$ :  $B_{\text{fast}}^{\text{total}} = \kappa_0^{\text{fast}} K_D^{\text{fast}}$ . 5) The buffering capacity of the fast buffer,  $\kappa_0^{\text{fast}}$ . Because the total buffering capacity is assumed to be fixed at 600, the capacity of the slow buffer is equal to  $600 - \kappa_0^{\text{fast}}$ . And 6) the distance from the exocytosis sensors to the center of the active zone,  $d^{XY}$ .

These parameters are summarized in Table 1. Dimensional stacking involves nesting simple two-dimensional parameter scans within each other with several parameters (in our case, 3) varied along each of the two axes. Each of the largest principal blocks, at the highest nesting level, is outlined with wider lines and corresponds to fixed values of the parameters labeled using the largest font-size ( $Q_{\text{Ca}}$  and  $K_D^{XY}$ ). Further, each of the major blocks consists of a grid of sub-blocks, corresponding to different values of parameters labeled with medium-sized font,  $D_B$  and  $K_D^{\text{fast}}$ . Finally, each of the sub-blocks presents a scan

over the values of two model parameters labeled with the smallest font,  $\kappa_0^{\text{fast}}$  and  $d^{XY}$ . Thus each square pixel in Fig. 6 corresponds to a particular choice of the values of six model parameters, which are given in Table 1. For each set of parameter values, a five-pulse simulation has been performed, and the point colored according to the following rule: 1) white (color-free) pixels correspond to parameters yielding five-pulse facilitation below the lower bound of  $R_5/R_1 = 14$ . 2) Pixel is colored gray if fura-2 reduces facilitation by  $<30\%$ . 3) Pixel is colored green if fura-2 reduces facilitation by  $>60\%$ . 4) Pixel is colored yellow if the reduction of facilitation by fura-2 is within the 30–60% range, consistent with experiment (Fig. 3A) but the delayed response 1 ms after the last pulse in the train is greater than the first control response. And 5) pixel is colored magenta if the delayed response is limited, the reduction of facilitation by fura-2 agrees with experiment, and the facilitation accumulation is super-linear. The corresponding parameter sets are deemed to satisfy the main experimental constraints. The parameter point corresponding to simulations in Figs. 2–5 lies within this region, and appears as a black pixel pointed to by a black arrow.

Note that facilitation is small (white regions) for small values of  $\text{Ca}^{2+}$  current and high buffer mobility because in this case, the endogenous buffers are able to absorb most of the  $\text{Ca}^{2+}$  influx before it reaches the facilitation sensor. Facilitation is also reduced due to the binding site saturation when the affinity of the  $\text{Ca}^{2+}$  binding gates is high ( $5 \mu\text{M}$ ) and the buffer concentration is low (recall that low  $B_{\text{fast}}^{\text{total}}$  corresponds to low  $K_D^{\text{fast}}$  because the buffer capacity is varied independently). The abundance of gray pixels at high values of  $\text{Ca}^{2+}$  influx is likewise easy to explain because for high  $Q_{\text{Ca}}$  values fura-2 cannot absorb a sufficient amount of  $\text{Ca}^{2+}$  influx to reduce facilitation. Similarly, the dominant green color on the left of Fig. 6 indicates a strong reduction of facilitation by fura-2 at low values of  $Q_{\text{Ca}}$ . The effect of other parameters on facilitation time course can be explained through similarly simple arguments.

#### DISCUSSION

We have shown that a model of synaptic response that relies on slow  $\text{Ca}^{2+}$  unbinding to explain synaptic facilitation is consistent with the properties of facilitation observed at the crayfish neuromuscular junction. Both the magnitude and the accumulation time course are successfully reproduced, and as demonstrated in Figs. 3 and 4, the model agrees with the observed reduction of facilitation on addition of fast exogenous  $\text{Ca}^{2+}$  buffers. In particular, the model response is decreased within milliseconds on adding  $200 \mu\text{M}$  of diazo-2-like buffer, consistent with experiments of Kamiya and Zucker (1994). The model indicates that introducing a fast exogenous buffer into a presynaptic terminal should affect not only the  $\text{Ca}^{2+}$ -dependent facilitation but also the baseline, unfacilitated neurotransmitter release. Our model captures both of these effects, predicting the reduction of binding of both the secretory X site as well as the slow-unbinding Y gates that are responsible for facilitation. This is because buffering will reduce the number of free  $\text{Ca}^{2+}$  ions reaching both of these sites, leading to reduced binding regardless of their kinetic properties. Therefore although experiments demonstrating a reduction in facilitation by exogenous buffers have been correctly interpreted to

show the importance of *free*  $\text{Ca}^{2+}$  dynamics during the induction of facilitation, we do not think those experiments rule out a role for accumulation of bound  $\text{Ca}^{2+}$ .

Thus we believe that facilitation due to slow  $\text{Ca}^{2+}$  unbinding is consistent with available data from the crayfish NMJ and may apply to other synapses as well. More specifically, the decay time course of facilitation may not be determined solely by the dynamics of intracellular  $\text{Ca}^{2+}$  diffusion and clearance but may depend on the intrinsic dynamics of the  $\text{Ca}^{2+}$ -binding sites involved in neurotransmitter release. This in fact is suggested by the experimentally observed discrepancy between the time scales of the decay of facilitation and the time scale of the concomitant decrease in intracellular  $[\text{Ca}^{2+}]$  (Atluri and Regehr 1996; Kamiya and Zucker 1994).

The present model, the previously proposed two-site mechanism (Matveev et al. 2002; Tang et al. 2000), and the buffer saturation model (Matveev et al. 2004; Neher 1998) can all successfully reproduce the magnitude and the time course of facilitation recorded in the crayfish inhibitor as well as the reduction of facilitation by fast  $\text{Ca}^{2+}$  buffers. However, the two-site model assumes that two spatially segregated  $\text{Ca}^{2+}$ -sensitive release gates control synaptic response, separated by distances of  $\geq 150$  nm. Further, to explain significant residual facilitation on application of  $\text{Ca}^{2+}$  indicator dye fura-2, the two-site model requires an assumption of strong immobilization of fura-2 by the cytoskeleton. In contrast, the bound- $\text{Ca}^{2+}$  mechanism described here assumes that the facilitation gates are co-localized with the  $\text{Ca}^{2+}$  binding site controlling phasic release and that mobile exogenous buffers remain mobile on injection into the terminal. Finally, the bound- $\text{Ca}^{2+}$  model is more successful than either of the two alternative mechanisms in reproducing the biphasic decay of facilitation.

Although we do not speculate on the physiological identity of the facilitation process, we note that the main feature of a model that includes a contribution of bound  $\text{Ca}^{2+}$  is that the underlying mechanism does *not* instantly re-equilibrate with the changing ambient  $\text{Ca}^{2+}$  concentration in contrast to any mechanism that is only sensitive to *free*  $\text{Ca}^{2+}$  accumulation. Therefore a bound  $\text{Ca}^{2+}$  model would arise naturally in describing processes characterized by nonnegligible time of reversal such as vesicle priming, which was recently proposed to underlie facilitation at the crayfish tonic synapses by Millar et al. (2005) (see also Bykhovskaia et al. 2004). In fact, the mechanism suggested by Millar et al. bears some similarity to our model but assumes that the fast secretory process and the facilitatory priming process characterized by slower kinetics operate sequentially rather than in parallel to each other and are spatially segregated as in the preceding-mentioned two-site model.

To conclude, we have demonstrated the viability of the residual bound  $\text{Ca}^{2+}$  hypothesis proposed by Katz and Miledi (1968) and Rahamimoff (1968). We have shown in particular that this model can account for facilitation at the crayfish NMJ. However, we do not exclude some contribution of free  $\text{Ca}^{2+}$  to facilitation in this preparation. In fact, the simulations in Figs. 2–5 would have revealed either free  $\text{Ca}^{2+}$  accumulation or  $\text{Ca}^{2+}$  transient growth due to buffer saturation had we chosen a somewhat different set of buffering parameters (within the optimal range shown in magenta in Fig. 6). Whereas free  $\text{Ca}^{2+}$  accumulation requires large concentrations of fixed buffers, facilitation of  $\text{Ca}^{2+}$  transients requires more mobile buffers

(Matveev et al. 2004). Although we did not optimize model parameters to exclude these two effects, the parameter combination that provided the best fit to all three experimental measures in Figs. 3–5 did not exhibit either of these two forms of free  $\text{Ca}^{2+}$  accumulation. Further, it is also possible that only one of the F1/F2 facilitation components is determined by the slow  $\text{Ca}^{2+}$  unbinding explored in this work, whereas the other component results from the effect of diffusion, buffering and/or  $\text{Ca}^{2+}$  clearance mechanisms on the free residual  $\text{Ca}^{2+}$ . Finally, we do not believe that accumulation of bound  $\text{Ca}^{2+}$  represents the primary mechanism of facilitation at *all* facilitatory synaptic terminals. Recent studies indicate that distinct cell types differentially express distinct facilitation mechanisms and that these may undergo differential regulation during development. For example, saturation of the endogenous buffer calbindin has been implicated in facilitation at calbindin-positive but not calbindin-negative mammalian central nerve terminals (Blatow et al. 2003), whereas the expression of calbindin is known to change during development (Alcantara et al. 1996). Furthermore, experimental evidence suggests that in some synapses facilitation involves a combination of mechanisms. For instance, both buffer saturation and accumulation of residual free  $\text{Ca}^{2+}$  were implicated in facilitation at the calyx of Held (Felmy et al. 2003) and at facilitatory calbindin-positive neocortical and hippocampal synapses (Blatow et al. 2003). We believe that at some synaptic terminals, such as the crayfish NMJ, residual bound  $\text{Ca}^{2+}$  provides an important contribution to synaptic facilitation.

Because all three mechanisms can account for the observed accumulation time course of synaptic facilitation, as well as its reduction by exogenous  $\text{Ca}^{2+}$  buffers, the question of the relative roles of free versus bound residual  $\text{Ca}^{2+}$  accumulation has to be addressed using more specific experimental protocols. One such method involves tracking the  $\text{Ca}^{2+}$  affinity of neurotransmitter release during induction of facilitation. If facilitation results solely from the build-up of *free* residual  $\text{Ca}^{2+}$ , the  $\text{Ca}^{2+}$  affinity of release should remain unchanged during stimulation because the state of the release machinery is not affected by stimulation under this assumption. This is indeed the case at the calyx of Held nerve terminals, as was shown by Felmy et al. (2003). If on the other hand there is an accumulation of  $\text{Ca}^{2+}$ -bound exocytosis gates during stimulation, the apparent  $\text{Ca}^{2+}$  affinity of exocytosis should increase as well because in this case, higher release probability is achieved despite the absence of a significant change in the  $\text{Ca}^{2+}$  concentration at the release site from one pulse to the next (cf. Fig. 3, B and C). Such a shift in the  $\text{Ca}^{2+}$  dependence of response would also manifest itself as an activity-dependent decrease in  $\text{Ca}^{2+}$  cooperativity (Stanley 1986). This is explained by the fact that less than four  $\text{Ca}^{2+}$  binding sites have to become bound to cause fusion on induction of facilitation because some of the Y sites will still be occupied by  $\text{Ca}^{2+}$  bound during the conditioning stimulation. Because such a shift in  $\text{Ca}^{2+}$  cooperativity was observed by Stanley (1986) at the squid giant synapse, there is a strong indication that bound  $\text{Ca}^{2+}$  is involved in facilitation in that preparation. We conclude that bound  $\text{Ca}^{2+}$  contributes to facilitation in some, but not all, synaptic terminals.

## ACKNOWLEDGMENTS

V. Matveev and R. Bertram acknowledge the hospitality of the Mathematical Biosciences Institute (OSU), where they have discussed some of the ideas presented in this manuscript.

## GRANTS

This work was supported by the National Science Foundation grants DMS-0417416 to V. Matveev and DMS-0311856 to R. Bertram and the Intramural Research Program of the National Institutes of Health, National Institute of Diabetes and Digestive and Kidney Disease to A. Sherman. The simulations were performed on the New Jersey Institute of Technology Hydra Beowulf cluster funded by National Science Foundation Grant MRI-0420590.

## REFERENCES

- Alcantara S, de Lacea L, Del Rio JA, Ferrer A, and Soriano E. Transient colocalization of parvalbumin and calbindin D28k in the postnatal cerebral cortex: evidence for a phenotypic shift in developing nonpyramidal neurons. *Eur J Neurosci* 8: 1329–1339, 1996.
- Allbritton NL, Meyer T, and Stryer L. Range of messenger action of calcium ion and inositol 1,4,5-trisphosphate. *Science* 258: 1812–1815, 1992.
- Atluri PP and Regehr WG. Determinants of the time course of facilitation at the granule cell to Purkinje cell synapse. *J Neurosci* 16: 5661–5671, 1996.
- Bennett MR, Farnell L, and Gibson WG. The facilitated probability of quantal secretion within an array of calcium channels of an active zone at the amphibian neuromuscular junction. *Biophys J* 86: 2674–2690, 2004.
- Bennett MR, Gibson WG, and Robinson J. Probabilistic secretion of quanta and the synaptosecretosome hypothesis: evoked release at active zones of varicosities, boutons, and endplates. *Biophys J* 73: 1815–1829, 1997.
- Bertram R, Sherman A, and Stanley E. The single domain/bound calcium hypothesis of transmitter release and facilitation. *J Neurophysiol* 75: 1919–1931, 1996.
- Bertram R, Swanson J, Yousef M, Feng ZP, and Zamponi GW. A minimal model for G protein-mediated synaptic facilitation and depression. *J Neurophysiol* 90: 1643–1653, 2003.
- Blatow M, Caputi A, Burnashev N, Monyer H, and Rozov A.  $\text{Ca}^{2+}$  buffer saturation underlies paired pulse facilitation in calbindin-D28k-containing terminals. *Neuron* 38: 79–88, 2003.
- Brody DL and Yue DT. Relief of G-protein inhibition of calcium channels and short-term synaptic facilitation in cultured hippocampal neurons. *J Neurosci* 20: 889–898, 2000.
- Bykhovskaia M, Polagaeva E, and Hackett JT. Mechanisms underlying different facilitation forms at the lobster neuromuscular synapse. *Brain Res* 1019: 10–21, 2004.
- Carafoli E. Intracellular calcium homeostasis. *Annu Rev Biochem* 56: 395–433, 1987.
- Chapman ER. Synaptotagmin: a  $\text{Ca}^{2+}$  sensor that triggers exocytosis? *Nat Rev Mol Cell Biol* 3: 498–508, 2002.
- Delaney KR and Tank DW. A quantitative measurement of the dependence of short-term synaptic enhancement on presynaptic residual calcium. *J Neurosci* 14: 5885–5902, 1994.
- Dipolo R and Beauge L. The calcium pump and sodium-calcium exchange in squid axons. *Annu Rev Physiol* 45: 313–324, 1983.
- Dittman JS, Kretzer AC, and Regehr WG. Interplay between facilitation, depression, and residual calcium at three presynaptic terminals. *J Neurosci* 20: 1374–1385, 2000.
- Felmy FE, Neher E, and Schneggenburger R. Probing the intracellular calcium sensitivity of transmitter release during synaptic facilitation. *Neuron* 37: 801–811, 2003.
- Fisher SA, Fischer TM, and Carew TJ. Multiple overlapping processes underlying short-term synaptic enhancement. *Trends Neurosci* 20: 170–177, 1997.
- Gabso M, Neher E, and Spira ME. Low mobility of the  $\text{Ca}^{2+}$  buffers in axons of cultured *Aplysia* neurons. *Neuron* 18: 473–481, 1997.
- Jackson MB and Redman SJ. Calcium dynamics, buffering, and buffer saturation in the boutons of dentate granule-cell axons in the hilus. *J Neurosci* 23: 1612–1621, 2003.
- Jeromin A, Shayan AJ, Msghina M, Roder J, and Atwood HL. Crustacean frequenins: molecular cloning and differential localization at neuromuscular junctions. *J Neurobiol* 41: 165–175, 1999.
- Kamiya H and Zucker RS. Residual  $\text{Ca}^{2+}$  and short-term synaptic plasticity. *Nature* 371: 603–606, 1994.
- Katz B and Miledi R. The role of calcium in neuromuscular facilitation. *J Physiol* 195: 481–92, 1968.
- Klingauf J and Neher E. Modeling buffered  $\text{Ca}^{2+}$  diffusion near the membrane: implications for secretion in neuroendocrine cells. *Biophys J* 72: 674–690, 1997.
- Koh TW and Bellen HJ. Synaptotagmin I, a  $\text{Ca}^{2+}$  sensor for neurotransmitter release. *Trends Neurosci* 26: 413–422, 2003.
- Lin JW, Fu Q, and Allana T. Probing the endogenous  $\text{Ca}^{2+}$  buffers at the presynaptic terminals of the crayfish neuromuscular junction. *J Neurophysiol* 94: 377–386, 2005.
- Maeda H, Ellis-Davies GC, Ito K, Miyashita Y, and Kasai H. Supralinear  $\text{Ca}^{2+}$  signaling by cooperative and mobile  $\text{Ca}^{2+}$  buffering in Purkinje neurons. *Neuron* 24: 989–1002, 1999.
- Magleby KL. Short-term changes in synaptic efficacy. In: *Synaptic Function*, edited by Edelman G, Gall W, and Cowan W. New York: Wiley, 1987, p. 21–56.
- Matveev V, Sherman A, and Zucker RS. New and corrected simulations of synaptic facilitation. *Biophys J* 83: 1368–1373, 2002.
- Matveev V, Zucker RS, and Sherman A. Facilitation through buffer saturation: constraints on endogenous buffering properties. *Biophys J* 86: 2691–2709, 2004.
- Millar AG, Zucker RS, Ellis-Davies GCR, Charlton MP, and Atwood HL. Calcium sensitivity of neurotransmitter release differs at phasic and tonic synapses. *J Neurosci* 25: 3113–3125, 2005.
- Neher E. Vesicle pools and  $\text{Ca}^{2+}$  microdomains: new tools for understanding their roles in neurotransmitter release. *Neuron* 20: 389–399, 1998.
- Nowycky MC and Pinter MJ. Time courses of calcium and calcium-bound buffers following calcium influx in a model cell. *Biophys J* 64: 77–91, 1993.
- Rahamimoff R. A dual effect of calcium ions on neuromuscular facilitation. *J Physiol* 195: 471–480, 1968.
- Regehr WG, Delaney KR, and Tank DW. The role presynaptic calcium in short-term enhancement at the hippocampal mossy fiber synapse. *J Neurosci* 14: 523–537, 1994.
- Rozov A, Burnashev N, Sakmann B, and Neher E. Transmitter release modulation by intracellular  $\text{Ca}^{2+}$  buffers in facilitating and depressing nerve terminals of pyramidal cells in layer 2/3 of the rat neocortex indicates a target cell-specific difference in presynaptic calcium dynamics. *J Physiol* 531: 807–826, 2001.
- Sala F and Hernández-Cruz A. Calcium diffusion modeling in a spherical neuron. Relevance of buffering properties. *Biophys J* 57: 313–324, 1990.
- Schmidt H, Stüefel KM, Racay P, Schwaller B, and Eilers J. Mutational analysis of dendritic  $\text{Ca}^{2+}$  kinetics in rodent Purkinje cells: role of parvalbumin and calbindin D28k. *J Physiol* 551: 13–32, 2003.
- Sippy T, Cruz-Martin A, Jeromin A, and Schweizer FE. Acute changes in short-term plasticity at synapses with elevated levels of neuronal calcium sensor-1. *Nat Neurosci* 6: 1006–1008, 2003.
- Stanley EF. Decline in calcium cooperativity as the basis of facilitation at the squid giant synapse. *J Neurosci* 6: 782–789, 1986.
- Tang Y, Schlumberger T, Kim T, Lueker M, and Zucker RS. Effects of mobile buffers on facilitation: experimental and computational studies. *Biophys J* 78: 2735–2751, 2000.
- Tank DW, Regehr WG, and Delaney KR. A quantitative analysis of presynaptic calcium dynamics that contribute to short-term enhancement. *J Neurosci* 15: 7940–7952, 1995.
- Taylor AL, Hickey TJ, Prinz AA, and Marder E. Structure and visualization of high-dimensional conductance spaces. *J Neurophysiol* 96: 891–905, 2006.
- Vyshedskiy A and Lin JW. Activation and detection of facilitation as studied by presynaptic voltage control at the inhibitor of the crayfish opener muscle. *J Neurophysiol* 77: 2300–2315, 1997.
- Yamada WM and Zucker RS. Time course of transmitter release calculated from simulations of a calcium diffusion model. *Biophys J* 61: 671–682, 1992.
- Zucker RS. Calcium- and activity-dependent synaptic plasticity. *Curr Opin Neurobiol* 9: 305–313, 1999.
- Zucker RS and Regehr WG. Short-term synaptic plasticity. *Annu Rev Physiol* 64: 355–405, 2002.